Human lateral Frontal Pole contributes to control over social-emotional action

Abbreviated title: FPl in social-emotional control

Bob Bramson[1], Davide Folloni[3,4], Lennart Verhagen[3,4], Bart Hartogsveld[5], Rogier B. Mars[1,4], Ivan Toni[1,*] and Karin Roelofs[1,2,*]

[1]Donders Institute for Brain, Cognition and Behavior, Centre for Cognitive Neuroimaging, Radboud University Nijmegen, 6525 EN Nijmegen, The Netherlands

[2]Behavioral Science Institute (BSI), Radboud University Nijmegen, 6525 HR Nijmegen, The Netherlands

[3]Wellcome Centre for Integrative Neuroimaging (WIN), Department of Experimental Psychology, University of Oxford, Oxford, OX1 3SR, United Kingdom

[4]Wellcome Centre for Integrative Neuroimaging (WIN), Centre for Functional MRI of the Brain (FMRIB), Nuffield Department of Clinical Neurosciences, John Radcliffe Hospital, University of Oxford, Oxford, OX3 9DU, United Kingdom

[5]Department of Clinical Psychological Science, Faculty of Psychology and Neuroscience, Maastricht University, 6229 ER Maastricht, The Netherlands

* These authors contributed equally

Conflicts declared: none.
Number of pages: 30
Number of figures: 3
Words abstract: 219
Words introduction: 650
Words discussion: 1489

Correspondence:
Bob Bramson
Donders Centre for Cognitive Neuroimaging
Radboud University Nijmegen
Trigon Building
Kapittelweg 29
6525 EN Nijmegen
The Netherlands
E-mail: b.bramson@donders.ru.nl

Acknowledgements: This work was supported by a VICI grant (#453-12-001) from the Netherlands Organization for Scientific Research (NWO) and a consolidator grant from the European Research Council (ERC_CoG-2017_772337) awarded to Karin Roelofs. The work of RBM is supported by the Netherlands Organization for Scientific Research (NWO) [452-13-015]. The work of DF was supported by Wellcome Trust UK Grant (105238/Z/14/Z).

Abstract

Regulation of emotional behavior is essential for human social interactions. Recent work has exposed its cognitive complexity, as well as its unexpected reliance on portions of the anterior prefrontal cortex (aPFC) also involved in exploration, relational reasoning, and counterfactual choice, rather than on dorsolateral and medial prefrontal areas involved in several forms of cognitive control. This study anatomically qualifies the contribution of aPFC territories to the regulation of social-emotional actions, and explores a possible structural pathway through which emotional regulation might be implemented.

We provide converging evidence from task-based fMRI, diffusion-weighted imaging, and functional connectivity fingerprints for a novel neural element in emotional regulation. Task-based fMRI in human male participants (N = 40) performing a social-emotional approach-avoidance task identified aPFC territories involved in the regulation of social-emotional actions. Connectivity fingerprints, based on diffusion-weighted imaging and resting-state connectivity, localized those task-defined frontal regions to the lateral frontal pole (FPl), an anatomically-defined portion of the aPFC that lacks a homologous counterpart in macaque brains. Probabilistic tractography indicated that 10-20% of inter-individual variation in social-emotional regulation abilities is accounted for by the strength of structural connectivity between FPl and amygdala. Evidence from an independent replication sample (N = 50; 10 females) further substantiated this result. These findings provide novel neuroanatomical evidence for incorporating FPl in models of control over human social-emotional behavior.

Keywords: social-emotional action control, amygdalofugal connectivity, prefrontal control, approach-avoidance, lateral frontal pole

Significance statement

Successful regulation of emotional behaviors is a prerequisite for successful participation in human society, as is evidenced by the social isolation and loss of occupational opportunities often encountered by people suffering from emotion-regulation disorders such as social-anxiety disorder and psychopathy. Knowledge about the precise cortical regions and connections supporting this control is crucial for understanding both the nature of computations needed to successfully traverse the space of possible actions in social situations, and the potential interventions that might result in efficient treatment of social-emotional disorders. This study provides evidence for a precise cortical region (FPl) and a structural pathway (the ventral amygdalofugal bundle) through which a cognitively complex form of emotional action regulation might be implemented in the human brain.

Introduction

Control of social-emotional behavior is paramount for successful participation in society (Hare, 2017). However, regulating social-emotional actions is cognitively complex. It requires the ability to assess the effectiveness of on-going behavior and compare this with alternative action strategies. For instance, a scientist presenting her work in front of a critical audience needs to overcome the tendency to avoid a potential criticism in order to reap the long-term benefits of peer-exposure and constructive feedback. Recent converging evidence indicates that this type of regulation of social-emotional behavior is implemented by the rostral part of the anterior prefrontal cortex (aPFC; Volman et al. 2011, 2013; Koch et al. 2018). The current study anatomically qualifies the contribution of aPFC regions to the regulation of social-emotional action, and explores a structural pathway through which this regulation might be implemented.

The aPFC has been involved in a disparate range of cognitive tasks, e.g. relational reasoning (Vendetti and Bunge, 2014; Hartogsveld et al., 2017), counterfactual choice (Boorman et al., 2009a; Mansouri et al., 2017), exploration behavior (Daw et al., 2006; Zajkowski et al., 2017). To date, emotional action regulation has not been considered part of the cognitive fingerprint of this region (Koch et al., 2018). Models of emotion regulation have predominantly focused on dorsolateral and medial prefrontal areas (Etkin et al., 2015; Morawetz et al., 2017; Langner et al., 2018). These models are largely based on explicit regulation strategies (e.g. reappraisal; Wager et al., 2008; Buhle et al., 2014) and have ignored control of emotional actions, an important component of emotion regulation concerned with conflict between the emotional value of stimulus and response (Frijda et al., 2014; Ridderinkhof, 2017; Bramson et al., 2018). At first glance, the focus of the emotion control literature on medial prefrontal cortex (mPFC) is justified by the strong structural and functional connectivity between mPFC and areas involved in emotional and social processing, such as the amygdala (Ghashghaei and Barbas 2002; Petrides and Pandya 2007; Neubert et al. 2014; Tillman et al. 2018). In contrast, structural connections to the amygdala are scarce for anterior prefrontal areas (Ghashghaei

et al., 2007). However, recent studies have shown that the amygdala is connected to the aPFC via rostral projections of the ventral amygdalofugal pathway (Krüger et al., 2015; Kamali et al., 2016). In fact, there is evidence that this tract might extend to the lateral frontal pole (FPl; Folloni et al., 2019), a portion of the human aPFC that does not have a homological counterpart in macaque brains (Neubert et al., 2014). These anatomical observations, together with converging functional evidence on aPFC involvement in the regulation of emotional strategies and actions (Bramson et al., 2018; Koch et al., 2018) raise the possibility that human social-emotional control is coordinated by the FPl.

In this study, we combine evidence from task-based fMRI, diffusion-weighted imaging, and resting-state connectivity fingerprints to define which portion of aPFC supports social-emotional control. First, we characterize the functional specificity of aPFC contributions to social-emotional control through a social-emotional approach-avoidance (AA) task. Participants approached or avoided happy and angry faces by means of speeded joystick reactions. Approaching angry and avoiding happy faces requires control over habitual social-emotional action tendencies, and elicits activity in aPFC (Roelofs et al., 2008; Volman et al., 2011b). The social relevance of the emotional-control indexed by this task has been established in social-emotional disorders (Bertsch et al., 2017; Volman 2016) and in healthy individuals where it predicted responses to real-life social stress-induction (Kaldewaij et al., 2019a). Second, we anatomically localize aPFC territories activated by the approach-avoidance task by matching structural and functional connectivity fingerprints of this area to fingerprints extracted from known areas of the aPFC (Neubert et al. 2014). Third, we assess the evidence for and the functional relevance of a structural pathway through which the portion of the aPFC activated by the AA task might support social-emotional regulation, namely through direct connections with the amygdala (Folloni et al., 2019).

Methods

Participants

Forty male students from the Radboud University Nijmegen participated in this study after giving informed consent. The sample had a mean age of 23.5 years (sd: 2.8, range 18-33 years). None of the participants reported history of mental illness or use of psychoactive/corticosteroid medication. All had normal or corrected to normal vision, and were screened for counter indications for magnetic resonance imaging (MRI). The study was approved by the local ethics committee (CMO:2014/288). Sample size was based on behavioral congruency effects observed previously in the same task (effect size *d = .4;* Volman et al, 2011). The sample consisted of males only in order to minimize potential variability caused by sex differences and fluctuations in cortisol and testosterone (e.g. due to different phases in the menstrual cycle). These hormones are known to influence behavioral and neural responses on the AA task (van Peer et al., 2007; Volman et al., 2011b; Kaldewaij et al., 2019a) and controlling for those fluctuations would have required a larger sample.

Given the novelty of one of the main findings of this report (correlation between amygdalofugal-FPl connectivity and behavioral congruency effect – see Results), we set out to replicate that finding in an independent convenience sample consisting of 50 participants [10 females, mean age = 23.8 (sd = 3.4, range 18-34)]. These participants took part in another study where they performed the AA task in a similar test-context, as well as a Diffusion weighted imaging (DWI) session. This second study was performed as part of a larger research project, after the analyses of the current study were finalized.

Materials and apparatus

Images were acquired using a 3T MAGNETROM Prisma MRI scanner (Siemens AG, Healthcare Sector, Erlangen, Germany) using a 32 channel headcoil for functional and DWI images and a 20 channel headcoil for structural T1 images. Stimuli were presented using an EIKI LC- XL100 beamer with a resolution of 1024 x 768 and a refresh rate of 60 Hz, and were projected onto a screen behind the scanner bore. Participants were able to see the screen via a mirror.

The approach-avoidance (AA) task consisted of 16 blocks of 12 trials each, in which participants had to approach or avoid equiluminant happy or angry faces presented in the centre of the screen. Faces were presented for 100 ms and preceded by a 500 ms fixation cross in the centre of the screen. After the presentation of the face, participants had 2000 ms to respond using a joystick. Each trial was followed by an intertrial interval of 2 – 4 seconds. Task instructions for congruent (move the joystick towards you/away from you for happy/angry faces), and incongruent blocks (move the joystick towards you/away from you for angry/happy faces), were presented before each block and switched between blocks. Subjects responded using a customized fiber optic response joystick, which was fixed to only move in the sagittal plane. Affect-incongruent trials have consistently been shown to activate the aPFC (Roelofs et al. 2008; Volman et al. 2011; Tyborowska et al. 2016; Kaldewaij et al., 2019). Behavioral and neural responses on this task are affected in several social-emotional disorders such as psychopathy, social-anxiety and borderline disorder (Heuer et al., 2007; von Borries et al., 2012; Roelofs and Cremers, 2015; Bertsch et al., 2018), and those responses are influenced by hormones affecting social behavior (Volman et al., 2016; Kaldewaij et al., 2019a).

Procedure

Data were acquired on two different days; day one consisted of the AA task, resting-state and T1 structural scan. DWI was acquired on the second day. Before and after the AA task we took saliva measurements to possibly control for testosterone and cortisol for other research purposes. On the second day, each participant filled out the State Trait Anxiety Inventory to control for effects of trait anxiety.

Functional scans

The field of view of the scans acquired in the two MR-sessions was aligned to a built-in brain-atlas using an auto-align head scout sequence. During resting state and task fMRI sessions we acquired BOLD-sensitive images using a multiband sequence with TR = 735 ms/TE = 39ms, 64 slices, flip angle of 52°, multiband acceleration factor of 8, slice orientation T > C, voxel size = 2.4 x 2.4 x 2.4

181 mm, phase encoding direction A >> P. The resting state session lasted 8.5 minutes (700 images). Each
182 sequence was followed by a field map image; flip angle = 60°, TR = 614, TE = 4.92.

183 *Structural scan*

184 High-resolution anatomical images were acquired with a single-shot MPRAGE sequence with
185 an acceleration factor of 2 (GRAPPA method), a TR of 2400 ms, TE 2.13 ms. Effective voxel size was 1
186 x 1 x 1 mm with 176 sagittal slices, distance factor 50%, flip angle 8°, orientation A ≫ P, FoV 256 mm.

187 *DW* imaging

188 Diffusion-weighted images were acquired using echo-planar imaging with an acceleration
189 factor of 2 (GRAPPA method). We acquired 65 2 mm-thick axial slices, with a voxel size of 2 x 2 x 2
190 mm, phase encoding direction A >> P, FoV 220 mm. In addition, we acquired 10 volumes without
191 diffusion weighting (b = 0 s/mm^2), 30 isotropically distributed directions using a b-value of 750
192 s/mm^2, and 60 isotropically distributed directions a b-value of 3000 s/mm^2. We also acquired a
193 volume without diffusion weighting with reverse phase encoding (P >> A).

194 Diffusion-weigthed images for the replication sample were acquired using echo-planar
195 imaging with multiband acceleration factor of 2 (GRAPPA method), multiband acceleration factor = 3.
196 For this dataset we acquired 93 1.6 mm thick transversal slices with voxel size of 1.6 x 1.6 x 1.6 mm,
197 phase encoding direction A >> P, FoV 211 mm, TR = 3350, TE = 71.20. 256 isotropically distributed
198 directions were acquired using a b-value of 2500 s/mm^2. We also acquired a volume without
199 diffusion weighting with reverse phase encoding (P >> A). Preprocessing and analyses for this dataset
200 were the same as for the original sample (reported below).

201 *Behavioral analyses*

202 Behavioral analyses of AA task performance contrasted incongruent to congruent trials,
203 comparing reaction times and percentage correct between conditions. Differences between
204 conditions were assessed using repeated measures ANOVA and paired-sample t-tests.

205 *Analyses - functional images*

206 All processing of the AA and resting state images was done using MELODIC 3.00 as
207 implemented in FSL 5.0.10 (https://fsl.fmrib.ox.ac.uk). Images were motion corrected using MCFLIRT
208 (Jenkinson et al., 2002), and distortions in the magnetic field were corrected using fieldmap
209 correction in FUGUE. Functional images were rigid-body registered to the brain extracted structural
210 image using FLIRT. Registration to MNI 2mm standard space was done using the nonlinear
211 registration tool FNIRT. Images were spatially smoothed using a Gaussian 5 mm kernel and low
212 passed filtered with a cut-off at 100 s. Independent component analysis was run (Beckmann and
213 Smith, 2004), after which the first 10 components were manually inspected to remove sources of
214 noise (Griffanti et al., 2017).

215 First and second level analyses were done in FEAT 6.00 implemented in FSL 5.0.10. We set up
216 separate general linear models for each task. The first-level AA model consisted of four task
217 regressors: Approach angry, approach happy, avoid angry and avoid happy; six motion regressors and
218 their temporal derivatives; and two regressors modeling fluctuations in signal in white matter and
219 cerebrospinal fluid. Approach happy and avoid angry (congruent conditions) were then contrasted
220 with approach angry and avoid happy (incongruent conditions). This contrast was taken as input for
221 each subject in the second level analysis. Second level analysis was performed using FMRIB's Local
222 Analysis of Mixed Effects (FLAME 1) with outlier de-weighting. We used a cluster forming threshold
223 of $Z > 2.3$, a value that has been shown to effectively control for Family Wise Error rate, possibly
224 related to the fact that FLAME estimates and takes into account within subject variance (Eklund et
225 al., 2015). Locations with above threshold activity were localized using masks for the prefrontal
226 cortex (Sallet et al., 2013; Neubert et al., 2014), parietal cortex (Mars et al., 2011) and whole brain
227 cortical and subcortical atlases (Harvard-Oxford atlas).

228 To assess psychophysiological interactions (PPI) during the AA task we ran a second analysis
229 using FEAT with regressors representing the task effects of interest (incongruent-congruent), the

230 regressor incongruent + congruent, a regressor describing the first eigenvariate time series of
231 activation of the seed region: Bilateral amygdalae taken from the AAL atlas (Tzourio-Mazoyer et al.,
232 2002), and a regressor describing the interaction between the seed region activity and task effects.
233 Strength of amygdalofugal-FPl connections as estimated from tractography of dw-MRI (see below)
234 was added as a covariate in the second level analysis.

235 *Analyses – functional connectivity fingerprints of FPl based on resting-state fMRI*

236 For the resting state fMRI analysis we defined regions-of-interest for each of the three areas
237 in aPFC (FPl, FPm, and 46), as identified by Neubert et al. (2014). These masks were thresholded to
238 contain only the 25% of voxels that were most likely to be part of each area (Mars et al., 2016;
239 Hartogsveld et al., 2017). The masks were warped to each individual anatomical space, after which
240 we extracted the first eigenvariate time series from each area. These time series were correlated
241 with whole brain resting state activity, the results of which were transformed to z-values using
242 Fishers z-transform and normalized. Resulting correlation maps were transformed back to MNI space
243 after which we extracted the connectivity from each prefrontal region with five downstream regions:
244 Posterior Cingulate Cortex (PCC) [10 -52 24], Intraparietal lobule (IPL) [48 -46 48], temporal pole (TP)
245 [34 12 -36], ventromedial prefrontal cortex (vmPFC) [8 44 -14] and dorsolateral prefrontal cortex
246 (dlPFC) [46 20 40], for each hemisphere separately. Differential connectivity with these five areas has
247 previously been shown to be appropriate to dissociate different cortical regions within aPFC (Mars et
248 al. 2016; Hartogsveld et al. 2017). This procedure creates a "connectivity fingerprint" of each region,
249 describing functional (and structural for DWI analyses) connections with other brain areas, and rests
250 on the premise that each regions' unique functional repertoire is determined by its connections with
251 other regions (Passingham et al., 2002; Mars et al., 2018). We followed the same procedure for the
252 two regions found in the aPFC during the AA task: 5 mm sphere around MNI [24 50 -4] and MNI [-24
253 52 4]. The focus of this study on aPFC responses to congruency demands during performance of the
254 AA task is related to a large body of work that has characterized and replicated those aPFC responses

255 across numerous studies (Roelofs et al., 2008; Volman et al., 2011a; Tyborowska et al., 2016). That
256 work has shown that activity in aPFC during incongruent trials is correlated with and necessary for
257 successfully overriding automatic action tendencies (Volman et al., 2011a); is influenced by several
258 neuromodulators such as testosterone and cortisol (van Peer et al., 2007; Volman et al., 2011b, 2016;
259 Kaldewaij et al., 2019a); is augmented in social psychopathology (von Borries et al., 2012; Radke et
260 al., 2013; Bertsch et al., 2017, 2018); and predicts real-world stress coping (Kaldewaij et al., 2019b).
261 The added value and validity of the structural explanation provided in the current study depends on
262 using the same functional comparison implemented in those previous studies, namely a direct
263 contrast between incongruent and congruent conditions.

264 For the statistical analysis, we computed the "city block" or "Manhattan" distance between
265 the connectivity profiles of the AA regions and the connectivity profiles of the three prefrontal
266 masks, separately for each hemisphere. This measure consists of the sum of absolute distance
267 between different connectivity profiles and has previously been used to describe the relative
268 dissimilarity between different connectivity profiles (Sallet et al., 2013; Neubert et al., 2014; Mars et
269 al., 2016). We compared these distance measures to a distribution of randomized distances that we
270 created by permuting the region labels 10000 times, each time randomly swapping the target region
271 labels (FPl; FPm; area 46) within participants and computing the Manhattan distance with the AA
272 fingerprint. The result of this approach shows whether the connectivity profile of the aPFC regions
273 differs from the connectivity profile of the region active during the AA task (Mars et al., 2016).

274 *Analyses – structural connectivity fingerprints of FPL based on diffusion-weighted MRI*

275 All analyses of diffusion data were performed in FSL FDT 3.0 (https://fsl.fmrib.ox.ac.uk). We
276 used TOPUP to estimate susceptibility artifacts using additional b = 0 volumes with reverse phase
277 coding direction (Andersson et al., 2003). Next, we used EDDY (using the fieldmap estimated by
278 TOPUP) to correct for distortions caused by eddy currents and subject movement (Andersson and

279 Sotiropoulos, 2016). We used BedpostX to fit a crossing fiber model using default settings (Behrens
280 et al., 2007).

281 Seed regions were defined for five major tracts by creating 5 mm spheres in the Cingulum
282 Bundle (CB) MNI: [8 -2 36], Superior Longitudinal Fasciculus 1 (SLF1), MNI: [16 -2 54], SLF 2, MNI: [30
283 -2 38], SLF 3, MNI: [44 -2 26] and Uncinate Fasciculus, MNI: [32 -2 -10] and then warped to individual
284 subject space. As with the functional connectivity described above, these specific fiber bundles were
285 chosen because they have been shown to be differentially connected to distinct areas within the
286 aPFC (Neubert et al., 2014; Mars et al., 2016; Hartogsveld et al., 2017). The procedure for
287 Amygdalofugal connectivity is described below. For the comparisons in the left hemisphere the same
288 coordinates were used with the x-axis coordinate inverted. ProbtrackX was run with default settings
289 using these masks as seed, separately for each hemisphere using an exclusion mask at x = 0. The
290 results from probtrackX were warped to MNI 1 mm space, log transformed, and normalized to the
291 highest probability per tract to allow a direct comparison between tracts with all values ranging
292 between 0 and 1. We computed connectivity profiles of FPl, FPm and area 46 by counting the
293 number of times each tract ended in these regions. These connectivity profiles were compared to the
294 connectivity profile of the region in the aPFC resulting from the AA task contrast (5 mm sphere at
295 MNI: [24 50 -4] for right and MNI: [-24 52 4] for left). We computed Manhattan distance between the
296 connectivity profiles of the AA task and the three prefrontal masks and permuted this 10,000 times,
297 each time randomly swapping the target region labels (FPl; FPm; area 46) within participants.

298 *Analyses - Amygdalofugal connectivity*

299 Connections between amygdala and aPFC were reconstructed using probtrackX. For this we
300 used the procedure and masks provided by Folloni et al., (2019). We seeded these connections in the
301 white matter punctuating the extended amygdala and substantia innominata: MNI: [-7 3 -9] and an
302 all-coronal waypoint mask at y = 22. We used tractography masks to ensure the estimated seedlines
303 extended only rostrally, at least up to the y = 25 coronal plane, and excluded CSF and between-

304 hemisphere connections. Connection strength was normalized and log transformed within each
305 participant. Next we extracted the total amount of times the tractography entered the FPl, FPm and
306 area 46 regions-of-interest separately. These values were correlated with congruency effects on
307 reaction time and percentage correct using Spearman's correlation coefficient.

308 To exclude that the Amygdalofugal-FPl connections are influenced by (much stronger)
309 projections of the Uncinate Fasciculus (UF), we reconstructed UF connectivity with FPl and correlated
310 this with the behavioral congruency. To isolate the UF we placed a seed in the white matter rostro-
311 laterally to the amygdala (MNI: [35 2 -22]), a coronal waypoint mask at y = 22 and exclusion masks in
312 the CSF and between hemispheres. We also used partial correlation to regress out possible
313 correlations influences of UF and state anxiety (STAI-Y2) in the amygdalofugal-behavioral
314 correlations. Finally, we used an independent comparison sample to confirm the correlation between
315 amygdalofugal-FPl connectivity and behavioral congruency.

316 **Results**

317 The study had two main goals: i) localize aPFC responses evoked during control over social-
318 emotional action tendencies in relation to an established anatomical parcellation of the aPFC; and ii)
319 provide evidence for the functional relevance of amygdala-aPFC connectivity in implementing control
320 over emotional-actions. We implemented a-priori determined analyses addressing these two goals,
321 correcting the statistical inferences for multiple comparisons, either through cluster correction (fMRI
322 task contrasts), or Bonferroni-correction (anatomical localization and tract-behavioral correlations).
323 Furthermore, we implemented a number of follow-up exploratory analyses, prioritizing sensitivity
324 over specificity, thus avoiding corrections for multiple comparisons. The exploratory nature of these
325 analyses is marked in the text.

326 *AA-task - Behavioral costs of controlling social-emotional behavior*

There were interaction effects between emotion and movement for reaction times; *F(1,39)* = 26.5, *p* < .001 and error rates; *F(1,39)* = 27.2, *p* < .001. Reaction times were longer for incongruent (M = 673 ms, SD = 103) than for congruent movements (M = 626 ms, SD = 128), *t*(39) = 5.12, *p* <.001 with an effect size of *d* = .4, CI [.22 , 1.03], calculated as (M1-M2) / sd_{pooled}]. Participants also made more errors during incongruent (M = 94.3 % correct, SD = 4.43) than congruent blocks (M = 97.1 % correct, SD = 2.96), *t*(39) = 5.21, *p < .001;* effect size *d* = .7, CI [.27 , 1.2]. In addition to these interaction effects there were main effects of movement *F(1,39)* = 32.9, *p* < .001; and emotion *F(1,39)* = 7.7, *p* = .008 on reaction times, but not on error rates, both *p* > .15. Approach movements were faster (M = 626 ms, SD = 106) then avoid movements (M = 661 ms, SD = 111) and reactions to happy faces (M = 635, SD = 103) were faster than to angry faces (M = 652, SD = 114). Interaction effects are depicted in figure 1B. These effects illustrate the behavioral cost of applying cognitive control over prepotent social-emotional action tendencies.

The replication sample also made more errors during incongruent (M= 94. 5 % correct) than in congruent trials (M = 96.8 % correct); *t*(49) = 6.25 *p* < .001.

AA-task - Controlling social-emotional actions elicits frontal and parietal activation

Building on previous evidence (Volman et al. 2011; Tyborowska et al. 2016), we expected that control over social emotional action tendencies increases aPFC activity. This study tests whether this activity can be localized to the lateral Frontal Pole. We found clusters of increased activity over frontal areas during incongruent as compared to congruent trials, whole-brain cluster-level corrected for multiple comparisons (cluster-forming threshold of Z > 2.3 with corrected cluster threshold of *p* < .05). Overlaying the frontal activity profiles on the mask created by Neubert et al. (2014) confirmed activity in FPl, figure 1C. In addition we observed clusters of increased activity in bilateral intraparietal lobule, an area strongly connected to the aPFC (Mars et al., 2011); bilateral Insula/Inferior Frontal Gyrus [34 26 -6]; Bilateral area 8A [40 6 42]; bilateral area 46 [30 50 16]; and bilateral cerebellum [16 -78 -30].

Contrasting happy and angry showed increased activity for happy trials in cerebellum [4 -62 -50], posterior cingulate [8 -48 24], anterior cingulate [-2 40 2] and lateral occipital cortex [30 -84 0]. Avoid trials showed increased activity in Frontal orbital cortex [44 20 -10] and occipital cortex: [32 -66 54].

The estimated BOLD signal indexing control over emotional action tendencies (incongruent vs congruent trials) extracted from FPl correlated positively with the behavioral index of emotional control (reaction time differences between incongruent and congruent trials): $r(38) = .33$, $p = .037$, figure 1D. This effect corroborates our earlier findings of a positive relationship between individual differences in reaction time effects and recruitment of aPFC/FPl activation (Roelofs et al. 2009; Bramson et al., 2018). Exploratory analyses correlating BOLD congruency with behavioral congruency gave a trend correlation for area 46; $r(38) = .31$, $p = .05$ and no correlation for FPm; $r(38) = .07$, $p = .63$. These correlations did not differ from the congruency-FPl correlation, both $p > .2$.

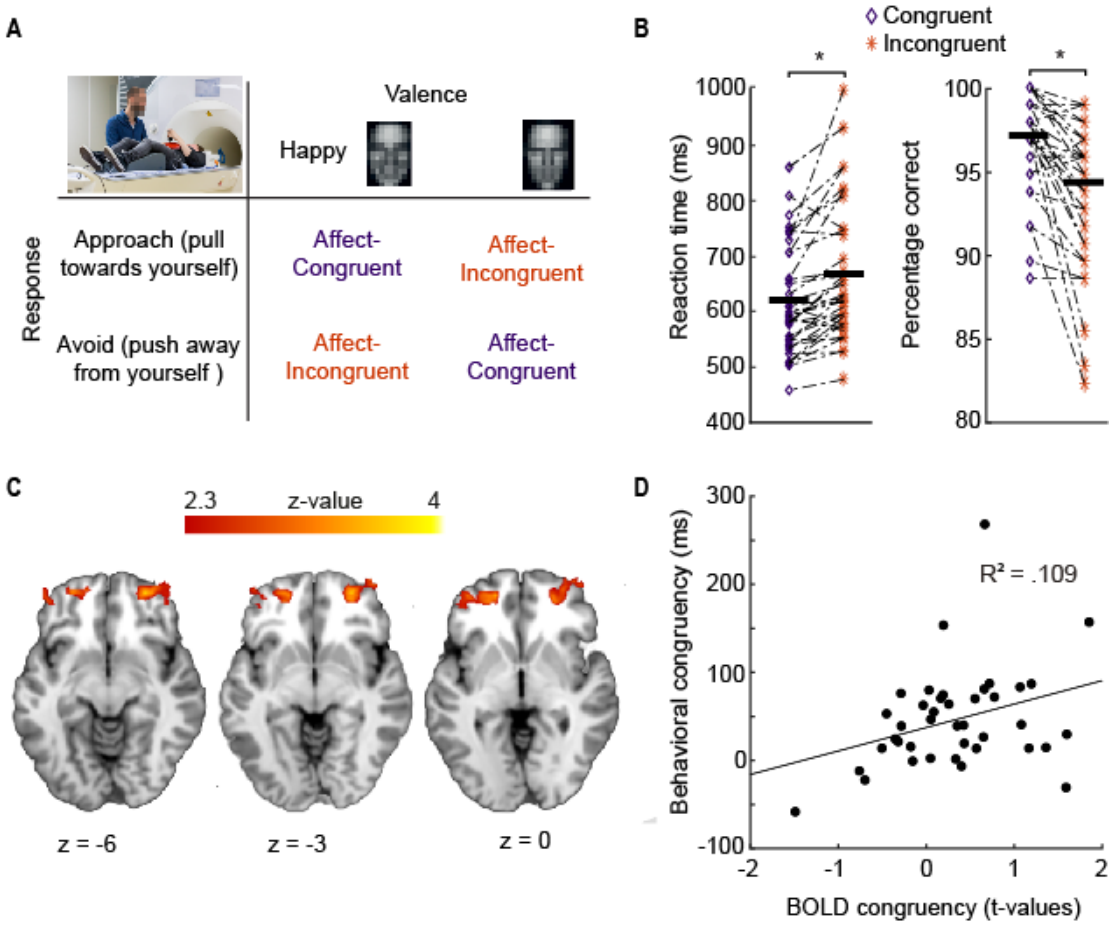

364

365 ***Figure 1: Effects of cognitive control over social-emotional action tendencies.***

366 *A) Schematic representation of the AA task used to measure control over social-emotional action*
367 *tendencies. The incongruent condition requires control to override the automatic tendencies to*
368 *approach happy- and avoid angry faces. B) Behavioral effects on AA task; participants show longer*
369 *reaction times and more errors during the incongruent condition, illustrating the cost of exerting*
370 *control. C) Main task effects for incongruent > congruent, masked to show above threshold (cluster*
371 *level p < .001) activation in the anterior Prefrontal Cortex. (Frontal Pole mask; Harvard-oxford atlas)*
372 *D) Correlation between reaction time congruency and BOLD congruency effects extracted from the*
373 *lateral Frontal Pole across participants.*

374

375

Relation between AA-related activity and functional fingerprints of FPl (Resting-state connectivity)

To assess whether the aPFC activity evoked during social-emotional control falls within FPl (Neubert et al. 2014), we compared resting-state connectivity profiles of area 46, FPl and FPm with the connectivity profile of the aPFC clusters showing a congruency effect (MNI: [24 50 -4] and [-24 52 -4]). We tested whether the connectivity fingerprints of the three prefrontal areas differed from the connectivity profile of the AA-related clusters, figure 2.

Qualitative inspection of the resting-state fingerprints showed relatively similar connectivity profiles for area 46 and FPl. Both are strongly correlated with the intraparietal sulcus (IPl) and dorsolateral prefontal cortex (dlPFC); however, FPl shows stronger connectivity to the posterior cingulate cortex (PCC). Functional connectivity of FPm differed quite strongly from both area 46 and FPl, showing strongest connectivity with ventromedial prefrontal areas (vmPFC), PCC and temporal pole (TP), figure 2A;C. These results corroborate earlier reports on resting-state connectivity fingerprints for these areas (Neubert et al., 2014; Mars et al., 2016; Hartogsveld et al., 2017).

Comparing connectivity profiles between the three areas in aPFC with the connectivity profile extracted from the AA-related region showed that its fingerprint differed significantly from that of area 46, (left hemisphere: $p < .001$; right-hemisphere: $p < .001$), and from that of area FPm (right hemisphere: $p < .001$; left-hemisphere: $p < .001$), but not from the connectivity fingerprint of area FPl (left-hemisphere: $p = .87$, right-hemisphere: $p = .075$). This result provides evidence that control of social emotional action tendencies involves the lateral Frontal Pole.

Relation between AA-related activity and structural fingerprints of FPl (DWI connectivity)

In addition to resting-state connectivity, we created connectivity profiles based on white matter tractography. We placed seeds in five large white matter tracts (figure 2B); performed probabilistic tractography to the rest of the hemisphere; and counted how often each tract ended in

399 each of the three regions in aPFC (figure 2B). We used a similar procedure for amygdalofugal (AmF)
400 connectivity (see methods).

401 Comparing connectivity profiles of the aPFC regions to these five major white matter tracts
402 and AmF connectivity showed relatively strong connectivity between area 46 and the three superior
403 longitudinal fasciculi (SLF1, SLF2 and SLF3; figure 2D). FPm is most strongly connected to the
404 Cingulate Bundle, Uncinate Fasciculus and Amygdalofugal pathways. FPl is less strongly connected to
405 the tracts leading outside the frontal cortex, and more strongly connected to the Uncinate Fasciculus,
406 which leads to the temporal pole (among other regions). The AA-related regions are also more
407 strongly connected to the Uncinate Fasciculus. These results are shown in figure 2D and match
408 earlier reports on connectivity of aPFC regions (Neubert et al., 2014; Mars et al., 2016; Hartogsveld et
409 al., 2017).

410 Comparing connectivity profiles between the three areas in aPFC with the connectivity
411 profile extracted from the AA region showed that the fingerprint of the AA region differed
412 significantly from that of area 46, (left hemisphere: $p < .001$; right-hemisphere: $p < .001$), and from
413 that of area FPm (right hemisphere: $p < .001$; left-hemisphere: $p < .001$), but not from the
414 connectivity fingerprint of area FPl (left-hemisphere: $p = .98$, right-hemisphere: $p = 1$). This result
415 corroborates the resting state results, providing additional evidence that the FPl is one of the regions
416 involved in controlling social emotional action tendencies.

417

418

419

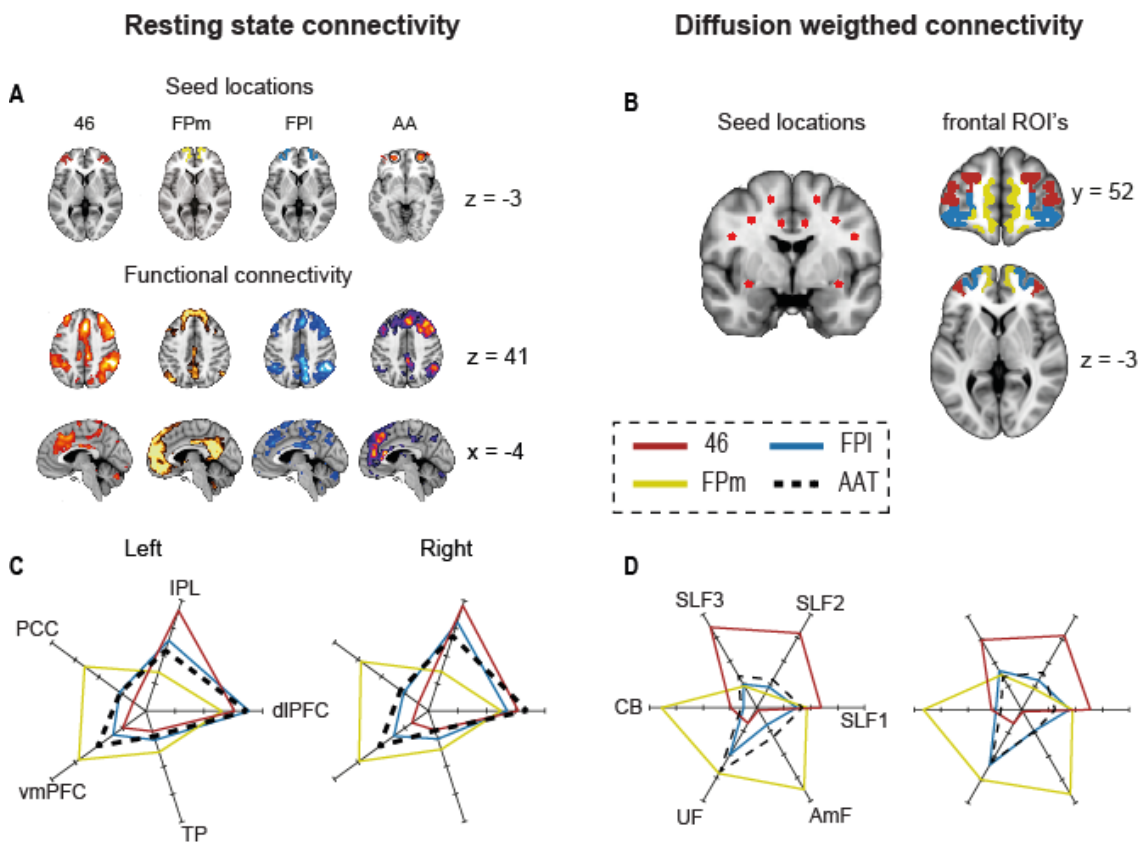

420

421 ***Figure 2: AA task effects are localized within the connectivity-defined lateral Frontal Pole.***

422 *A) Seed regions and whole brain resting-state connectivity for area 46, FPm, FPl, and for the cluster*
423 *showing AA task-effects. B) Seed locations for tractography in five large white matter tracts (AmF*
424 *seed not shown) and masks for the regions FPl, FPm and area 46. C) Resting state connectivity*
425 *fingerprints of the aPFC and AA regions, separated for left and right ROI's. Region labels: Posterior*
426 *Cingulate Cortex (PCC), ventromedial prefrontal cortex (vmPFC), Intraparietal Lobule (IPL),*
427 *dorsolateral Prefrontal Cortex (dlPFC), Temporal Pole (TP). D) Connectivity fingerprints for*
428 *tractography of aPFC and the AA regions, separated for left and right ROI's. Tract abbreviations:*
429 *Superior Longitudinal Fasciculus (SLF1, SLF2, SLF3); Uncinate Fasciculus (UF); Cingulum Bundle (CB);*
430 *Amygdalofugal (AmF).*

431

432

FPl-amygdalofugal connectivity partly explains performance on the AA task.

To identify an anatomical pathway through which the FPl could support social-emotional behavior, we tested whether inter-subject variability in the strength of FPl structural connectivity mediated by the amygdalofugal connections predicts successful performance on the AA task. On average, the FPm is more strongly connected to amygdalofugal pathways than the FPl and area 46 (Figure 3A), in line with earlier studies showing both functionally and anatomically stronger connections between limbic areas and medial prefrontal regions (Ghashghaei and Barbas, 2002; Neubert et al., 2014; Folloni et al., 2019). However, individual variability in the connectivity of FPl and FPm confirms that the former region is more strongly involved in social-emotional control than the latter. Namely, there was a significant correlation between tract strength and AA congruency effect on percentage correct; Spearman's $r(38)$ .44 =, p = .004 for the FPl connections but not for FPm, $r(38)$ = .24, p = .13 and area 46, $r(38)$ = .3, p = .062, figure 3B. However, these correlations did not differ from one another, both comparisons $p > .3$. The direction of the FPl-behavioral correlation indicated that stronger connectivity was related to relatively worse performance when having to exert control. There were no significant correlations between tract strength and congruency effect on reaction time; all $p > .09$. The congruency-FPl correlation for percentage correct survives Bonferroni-correction for multiple comparisons over the eight correlations computed between behavioral congruency and amygdalofugal-FPl connectivity; and the two control correlations described below.

To facilitate data interpretation, we conducted 2 additional exploratory control analyses. First, to exclude that the correlation between amygdalofugal-FPl connectivity and AA performance could be better explained by connections between amygdala and FPl through the Uncinate Fasciculus (UF; Petrides and Pandya 2007) or trait anxiety (Kim and Whalen, 2009), we correlated UF-FPl connectivity with AA performance, and amygdalofugal-FPl connectivity with scores on the State anxiety inventory (STAI). None of these analyses yielded significant correlations, all $p > .58$. Nor did

458 the correlation between amygdalofugal-FPl connections and behavioral congruency change when
459 controlling for state anxiety or UF-FPl connectivity.

460 Second, to explore whether FPl-amygdalofugal connectivity would also influence functional
461 connectivity between these two areas, we performed a Psychophysiological Interaction (PPI) analysis
462 with bilateral amygdalae as seed region and the strength of the connection with FPl as covariate. This
463 analysis showed a negative correlation between tract strength and amygdala-FPl functional
464 connectivity during the task, when using a small volume correction over bilateral FPl; $p = .019$ (FWE
465 cluster corrected; cluster location MNI [-32 50 6], cluster size: 20 voxels), meaning that with
466 increased tract strength there is more negative connectivity between the FPl and amygdala, which
467 might be interpreted as increased regulation of amygdala by the FPl (Volman et al., 2013).

468 Finally, given the novelty of the role of the amygdalofugal path in emotion control, we tested
469 whether the correlation between behavioral congruency and amygdalofugal connectivity would
470 replicate in an independent sample of 50 participants. The positive relationship between the
471 congruency effect in % correct on the AA task and amygdalofugal-FPl connections was confirmed;
472 Spearman's $r(48) = .3$, $p = .03$, figure 3C, further substantiating this finding.

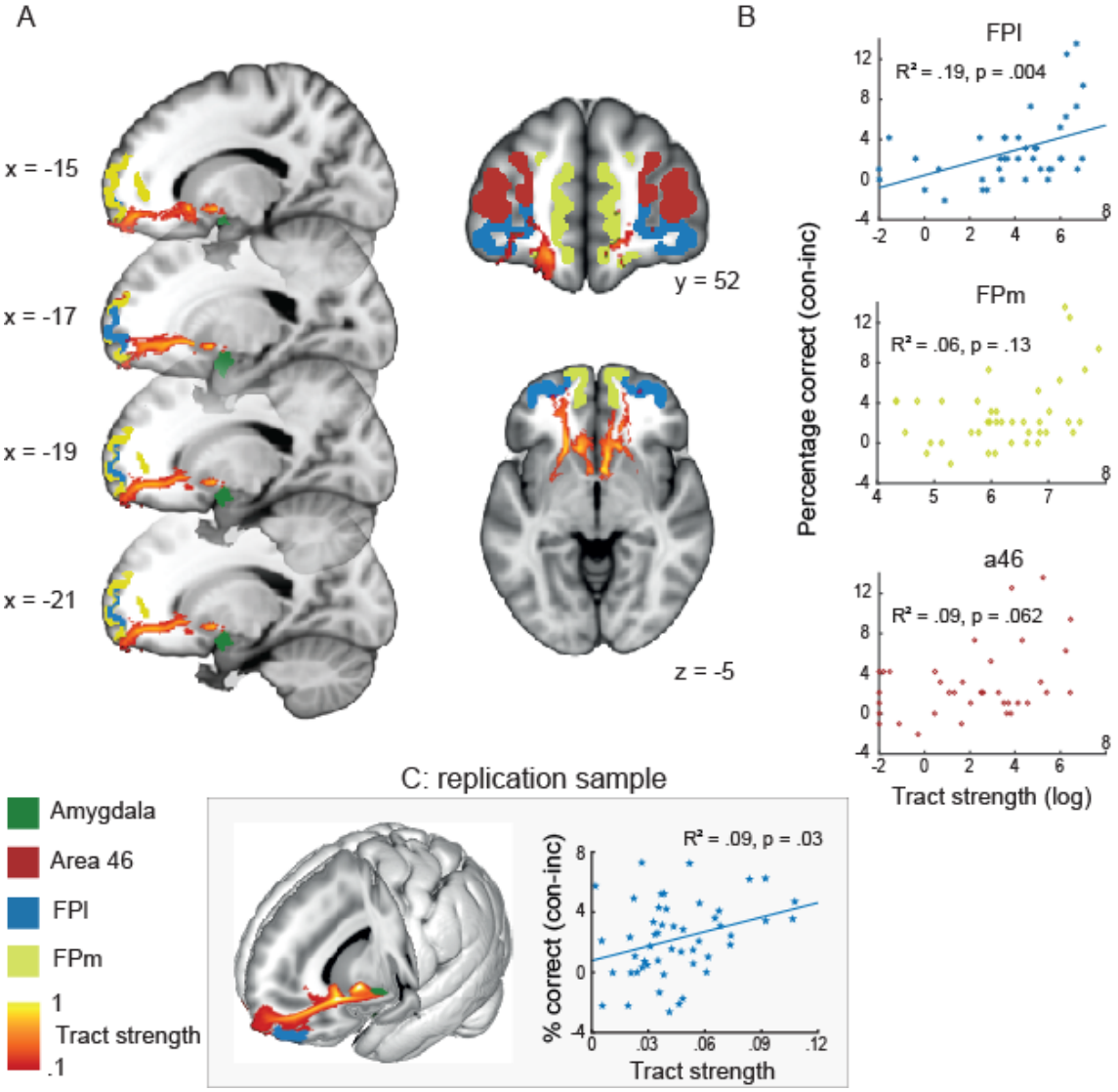

Figure 3: Amygdalofugal connections with FPl correlate with AA task performance.

A) Illustration of the reconstructed tract that leads from the Amygdala to the anterior Prefrontal cortex. This tract shows strongest connectivity with medial prefrontal areas, as can be expected given earlier studies. B) The number of times the tract ends in FPl correlates with behavioral congruency in error rates on the AA task, r = .44, p = .0044, suggesting that the amygdalofugal pathway is involved in mediating FPl-amygdala functional interactions during social-emotional control. C) Illustration of the reconstructed tract and correlation between behavioral congruency and tract strength with FPl in the replication sample.

482 **Discussion**

483 The present study anatomically qualifies the involvement of the anterior prefrontal cortex in
484 social-emotional action control. There are two main findings. First, structural and functional
485 connectivity fingerprints of the lateral Frontal Pole (Neubert et al., 2014) closely match the
486 fingerprints of the aPFC territory recruited when social-emotional control is required. Second, the
487 strength of FPl structural connectivity with the amygdala accounts for a substantial portion of inter-
488 individual variation in social-emotional regulation abilities. These findings provide evidence for a
489 precise cortical region (FPl) and a structural pathway (the ventral amygdalofugal bundle) through
490 which a cognitively complex form of emotional regulation might be implemented in the human brain.

491 **FPl supports social-emotional control**

492 Previous work has repeatedly shown that the aPFC is involved in controlling social-emotional
493 behavior, and that it is capable of doing so by influencing downstream activity in the amygdala
494 (Volman et al. 2013; Tyborowska et al. 2016); motor cortex; and parietal areas (Volman et al. 2011;
495 Bramson et al. 2018). Here, we extend this knowledge by showing that the aPFC contribution to
496 social-emotional control arises from a precise anatomical structure: the lateral Frontal Pole (Neubert
497 et al., 2014). This finding is based on the connectivity fingerprint of the FPl. This anatomical metric
498 also provides clues to the information received by the FPl, and the influence it can exert on other
499 brain structures (Mars et al., 2018). The FPl, differently from neighbouring areas FPm and 46, is
500 connected to both medial and lateral circuits with parietal, cingulate, and temporal regions (Figure
501 2). The peculiar pattern of FPl connectivity fits with the known supramodal regulatory role of this
502 area during social-emotional control (Volman et al. 2011; Volman et al. 2013; Koch et al. in prep), and
503 with the notion that social-emotional regulation involves access to both egocentric value of
504 emotionally-laden actions, as well as social consequences of those actions (Koch et al., 2018).

505 This study was designed to add functional specificity to those anatomically-grounded
506 inferences on aPFC contributions to social-emotional regulations. The observations of this study link

507 social-emotional regulation to several cognitive processes that rely on the FPl, e.g. concurrent
508 monitoring of current and alternative goals (Burgess et al., 2007; Badre and D'esposito, 2009;
509 Mansouri et al., 2017), cognitive exploration (Daw et al., 2006; Zajkowski et al., 2017), counterfactual
510 reasoning (Boorman et al., 2009b; Koechlin, 2016), metacognition (Fleming et al., 2014; Shekhar and
511 Rahnev, 2018), and relational reasoning (Vendetti and Bunge, 2014; Hartogsveld et al., 2017). More
512 precisely, it becomes relevant to test whether the FPl contribution to social-emotional control is
513 linked to the online maintenance and evaluation of alternative goals or counterfactual regulation
514 strategies (Sheppes et al., 2014; Koch et al., 2018); or whether the cognitive demands of social-
515 emotional control and their input-output connectivity segregate this faculty from other known FPl
516 functions.

517 **Amygdala-FPl projections modulate control over emotional-action**

518 This study shows that control over social-emotional actions is negatively associated with the
519 strength of amygdala-FPl connections, with connections between amygdala and FPl explaining over
520 20% of the variance on the AA task. This result was confirmed in an independent replication sample.
521 On the assumption that the amygdala-FPl connectivity indexed in this study captures the
522 amygdalofugal pathway (Folloni et al. 2019), i.e. the main efferent pathways from amygdala to
523 frontal cortex (Nolte, 1999; Ghashghaei and Barbas, 2002; Noback et al., 2005; Krüger et al., 2015;
524 Kamali et al., 2016), this finding suggests that stronger amygdala projections to the FPl impair
525 emotional regulation. Namely, during incongruent trials, stronger amygdala afferences to the FPl
526 could lead to stronger automatic action tendencies or heightened emotional vigilance and thus more
527 errors when those tendencies need to be rapidly over-ruled. This observation fits with previous
528 imaging work showing that successful emotional control reduces bottom-up effective connectivity
529 between amygdala and aPFC (Volman et al., 2013). Moreover, it suggests that top-down regulatory
530 FPl efferences might reach the amygdala through other fiber bundles, e.g. the uncinate fasciculus

531 (Petrides and Pandya, 2007; Folloni et al., 2019); or through other regions, e.g. the nucleus
532 accumbens (Wager et al., 2008) or the orbitofrontal cortex (Ray and Zald, 2012).

533 The relation between amygdala-FPl connectivity strength and social-emotional action control
534 observed in this study is surprisingly large when compared to the magnitude of previous structure-
535 function correlations in the same anatomical regions (Jung et al., 2018). We suspect that the large
536 effect size is a consequence of considering the anatomical differences between fiber bundles
537 connecting the amygdala to the prefrontal cortex, and in particular the uniquely human configuration
538 of that connectivity, since anthropoid monkeys do not possess a functional homologue of the human
539 lateral Frontal Pole (Semendeferi et al., 2010; Neubert et al., 2014; Mars et al., 2016). Future tests of
540 this potential functional-anatomical dissociation between bottom-up and top-down amygdala-FPl
541 connectivity might also help to clarify the heterogeneity of previous findings concerning the relation
542 between amygdala-prefrontal connectivity and state-anxiety measures (Kim and Whalen, 2009;
543 Clewett et al., 2014).

544 **Interpretational issues**

545 It could be argued that the regulation required in the AA task is just an instance of inhibitory
546 control with social stimuli, and that regulation in this task could be accomplished by suppressing
547 automatic emotional action tendencies (Etkin et al., 2006; Aron et al., 2014). Several studies have
548 shown that this is not a viable option. First, when participants respond to the gender rather than the
549 emotion of the face, both behavioral (congruency effect) and neural correlates of emotional control
550 (FPl activation) are extinguished (Roelofs et al., 2008; Volman et al., 2011b). This illustrates that the
551 regulation indexed by the AA task crucially depends on the interaction between emotional percepts
552 and action selection, rather than on overriding conflict contained in the stimulus itself (e.g.
553 emotional Stroop task, which is supported by different neural circuitry (Etkin et al., 2011, 2015)).
554 Second, performance on the AA task is specifically altered in patients with disrupted social-emotional
555 regulation (Heuer et al., 2007; van Peer et al., 2009; von Borries et al., 2012). For instance,

556 aggression-related psychopathologies such as psychopathy are marked by reduction of avoidance
557 responses, specific to angry faces, an effect related to measures of social aggression (von Borries et
558 al., 2012). In contrast, patients with social anxiety disorder show a consistent increase of avoidance
559 responses, specific to angry faces (Roelofs et al., 2005, 2009, 2010; Heuer et al., 2007). In addition,
560 socially-relevant hormones such as testosterone (Tyborowska et al., 2016), cortisol (Volman et al.,
561 2011b), and oxytocin (Radke et al., 2017) influence performance of the Approach-Avoidance task in
562 healthy participants. Most critically, the aPFC congruency effect measured during the social
563 approach-avoidance task is predictive of subjective, physiological and hormonal responses to a real-
564 life social stressor (Kaldewaij et al., 2019b). In sum, these studies highlight the validity of the AA task
565 for indexing social-emotional regulation.

566 In principle, the relation between strength of amygdala-FPl connectivity and behavioral
567 emotional control could be explained by a third factor, e.g. trait anxiety. However, the tract strength
568 between amygdala and FPl did not correlate with trait anxiety, and the correlation between
569 behavioral congruency and tract strength persisted when controlling for anxiety. This observation
570 confirms that, in healthy participants, aPFC activity during the AA task is orthogonal to trait anxiety
571 effects (Bramson et al., 2018), in contrast to known trait anxiety effects on amygdala-vmPFC
572 connectivity (Kim and Whalen, 2009).

573 It is not easy to acquire reliable fMRI signals from anterior prefrontal regions (Hutton et al.,
574 2002). Therefore, we used magnetic field corrections to restore signal distortions around the frontal
575 pole (Jezzard and Balaban, 1995; Jenkinson, 2004). The resting-state connectivity profiles closely
576 matched those of earlier studies that used different MRI protocols (Neubert et al., 2014; Mars et al.,
577 2016) arguing against the possibility that the results reported here can be attributed to signal
578 distortions. The first sample of participants consisted of males only, and the replication sample was
579 predominantly male. Whereas behavioral and neural effects in the AA task have been shown in
580 mixed and female only samples as well (Radke et al., 2015; Tyborowska et al., 2016; Bertsch et al.,

581 2018), we recruited only males to avoid having to control for differences in social hormones such as
582 testosterone and cortisol, which would require a larger sample of participants. These hormones are
583 known to influence behavioral and neural responses on the AA task (van Peer et al., 2007; Volman et
584 al., 2011b; Kaldewaij et al., 2019a). Future studies could explore similarities and potential differences
585 in emotional processing between sexes (Domes et al., 2010; Whittle et al., 2011).

586 **Conclusion**

587 This study provides anatomical evidence supporting the involvement of the lateral frontal
588 pole, partly via the ventral amygdalofugal pathway, in the regulation of social-emotional behavior
589 (Koch et al., 2018). The findings have implications for structuring mechanism-based interventions in
590 psychopathologies characterized by altered emotional control abilities, e.g. anxiety disorders and
591 psychopathy (Volman et al., 2016). The findings are also relevant for understanding the
592 neurobiological and cognitive complexities underlying rule-based regulation of action tendencies,
593 arguably a crucial pre-requisite for the development of human cumulative culture (Hare, 2017;
594 Whiten, 2017).

595

596

597

598

599 **References**

600 Andersson JLR, Skare S, Ashburner J (2003) How to correct susceptibility distortions in spin-echo
601 echo-planar images: application to diffusion tensor imaging. Neuroimage 20:870–888.

602 Andersson JLR, Sotiropoulos SN (2016) An integrated approach to correction for off-resonance
603 effects and subject movement in diffusion MR imaging. Neuroimage 125:1063–1078.

604 Aron AR, Robbins TW, Poldrack RA (2014) Inhibition and the right inferior frontal cortex: one decade
605 on. Trends Cogn Sci 18:177–185.

606 Badre D, D'esposito M (2009) Is the rostro-caudal axis of the frontal lobe hierarchical? Nat Rev
607 Neurosci 10:659–669.

608 Beckmann CF, Smith SM (2004) Probabilistic independent component analysis for functional
609 magnetic resonance imaging. IEEE Trans Med Imaging 23:137–152.

610 Behrens TEJ, Berg HJ, Jbabdi S, Rushworth MFS, Woolrich MW (2007) Probabilistic diffusion
611 tractography with multiple fibre orientations: What can we gain? Neuroimage 34:144–155.

612 Bertsch K, Roelofs K, Roch PJ, Ma B, Hensel S, Herpertz SC, Volman I (2018) Neural correlates of
613 emotional action control in anger-prone women with borderline personality disorder. J
614 psychiatry Neurosci JPN 43:170102.

615 Bertsch K, Volman I, Roelofs K, Herpertz SC, Müller LE (2017) Social emotional leaning and behavioral
616 tendencies in high and low socially anxious men and women. Psychoneuroendocrinology 83:49.

617 Boorman ED, Behrens TEJ, Woolrich MW, Rushworth MFS (2009a) How Green Is the Grass on the
618 Other Side? Frontopolar Cortex and the Evidence in Favor of Alternative Courses of Action.
619 Neuron 62:733–743 Available at: http://dx.doi.org/10.1016/j.neuron.2009.05.014.

620 Boorman ED, Behrens TEJ, Woolrich MW, Rushworth MFS (2009b) How green is the grass on the
621 other side? Frontopolar cortex and the evidence in favor of alternative courses of action.
622 Neuron 62:733–743.

623 Bramson B, Jensen O, Toni I, Roelofs K (2018) Cortical oscillatory mechanisms supporting the control
624 of human social-emotional actions. J Neurosci:3317–3382.

625 Buhle JT, Silvers JA, Wager TD, Lopez R, Onyemekwu C, Kober H, Weber J, Ochsner KN (2014)
626 Cognitive reappraisal of emotion: a meta-analysis of human neuroimaging studies. Cereb cortex

627 24:2981–2990.

628 Burgess PW, Dumontheil I, Gilbert SJ (2007) The gateway hypothesis of rostral prefrontal cortex (area
629 10) function. Trends Cogn Sci 11:290–298.

630 Daw ND, O'doherty JP, Dayan P, Seymour B, Dolan RJ (2006) Cortical substrates for exploratory
631 decisions in humans. Nature 441:876–879.

632 Domes G, Schulze L, Böttger M, Grossmann A, Hauenstein K, Wirtz PH, Heinrichs M, Herpertz SC
633 (2010) The neural correlates of sex differences in emotional reactivity and emotion regulation.
634 Hum Brain Mapp 31:758–769.

635 Eklund A, Nichols T, Knutsson H (2015) Can parametric statistical methods be trusted for fMRI based
636 group studies? Proc Natl Acad Sci 113:7900–7905 Available at:
637 http://arxiv.org/abs/1511.01863%0Ahttp://dx.doi.org/10.1073/pnas.1602413113.

638 Etkin A, Büchel C, Gross JJ (2015) The neural bases of emotion regulation. Nat Rev Neurosci 16:693.

639 Etkin A, Egner T, Kalisch R (2011) Emotional processing in anterior cingulate and medial prefrontal
640 cortex. Trends Cogn Sci 15:85–93.

641 Etkin A, Egner T, Peraza DM, Kandel ER, Hirsch J (2006) Resolving emotional conflict: a role for the
642 rostral anterior cingulate cortex in modulating activity in the amygdala. Neuron 51:871–882.

643 Fleming SM, Ryu J, Golfinos JG, Blackmon KE (2014) Domain-specific impairment in metacognitive
644 accuracy following anterior prefrontal lesions. Brain 137:2811–2822.

645 Folloni D, Sallet J, Khrapitchev AA, Sibson N, Verhagen L, Mars RB (2019) Dichotomous organization
646 of amygdala/temporal-prefrontal bundles in both humans and monkeys Heilbronner S, Gold JI,
647 Thiebaut de Schotten M, eds. Elife 8:e47175.

648 Frijda NH, Ridderinkhof KR, Rietveld E (2014) Impulsive action: emotional impulses and their control.

649 Front Psychol 5:518.

650 Ghashghaei HT, Barbas H (2002) Pathways for emotion: interactions of prefrontal and anterior
651 temporal pathways in the amygdala of the rhesus monkey. Neuroscience 115:1261–1279.

652 Ghashghaei HT, Hilgetag CC, Barbas H (2007) Sequence of information processing for emotions based
653 on the anatomic dialogue between prefrontal cortex and amygdala. Neuroimage 34:905–923.

654 Griffanti L, Douaud G, Bijsterbosch J, Evangelisti S, Alfaro-Almagro F, Glasser MF, Duff EP, Fitzgibbon
655 S, Westphal R, Carone D (2017) Hand classification of fMRI ICA noise components. Neuroimage
656 154:188–205.

657 Hare B (2017) Survival of the friendliest: Homo sapiens evolved via selection for prosociality. Annu
658 Rev Psychol 68:155–186.

659 Hartogsveld B, Bramson B, Vijayakumar S, van Campen AD, Marques JP, Roelofs K, Toni I, Bekkering
660 H, Mars RB (2017) Lateral frontal pole and relational processing: Activation patterns and
661 connectivity profile. Behav Brain Res.

662 Heuer K, Rinck M, Becker ES (2007) Avoidance of emotional facial expressions in social anxiety: The
663 Approach–Avoidance Task. Behav Res Ther 45:2990–3001.

664 Hutton C, Bork A, Josephs O, Deichmann R, Ashburner J, Turner R (2002) Image distortion correction
665 in fMRI: a quantitative evaluation. Neuroimage 16:217–240.

666 Jenkinson M (2004) Improving the registration of B0-distorted EPI images using calculated cost
667 function weights. In: Tenth International Conference on functional mapping of the human brain.

668 Jenkinson M, Bannister P, Brady M, Smith S (2002) Improved optimization for the robust and
669 accurate linear registration and motion correction of brain images. Neuroimage 17:825–841.

670 Jezzard P, Balaban RS (1995) Correction for geometric distortion in echo planar images from B0 field

variations. Magn Reson Med 34:65–73.

Kaldewaij R, Koch SBJ, Zhang W, Hashemi MM, Klumpers F, Roelofs K (2019a) High endogenous testosterone levels are associated with diminished neural emotional control in aggressive police recruits. Psychol Sci:0956797619851753.

Kaldewaij R, Koch SBJ, Zhang W, Hashemi MM, Klumpers F, Roelofs K (2019b) Frontal control over automatic emotional action tendencies predicts acute stress responsivity. Biol Psychiatry Cogn Neurosci Neuroimaging.

Kamali A, Sair HI, Blitz AM, Riascos RF, Mirbagheri S, Keser Z, Hasan KM (2016) Revealing the ventral amygdalofugal pathway of the human limbic system using high spatial resolution diffusion tensor tractography. Brain Struct Funct 221:3561–3569.

Kim MJ, Whalen PJ (2009) The structural integrity of an amygdala–prefrontal pathway predicts trait anxiety. J Neurosci 29:11614–11618.

Koch SBJ, Mars RB, Toni I, Roelofs K (2018) Emotional control, reappraised. Neurosci Biobehav Rev 95:528–534 Available at: https://linkinghub.elsevier.com/retrieve/pii/S0149763418301672.

Koechlin E (2016) Prefrontal executive function and adaptive behavior in complex environments. Curr Opin Neurobiol 37:1–6.

Krüger O, Shiozawa T, Kreifelts B, Scheffler K, Ethofer T (2015) Three distinct fiber pathways of the bed nucleus of the stria terminalis to the amygdala and prefrontal cortex. Cortex 66:60–68.

Langner R, Leiberg S, Hoffstaedter F, Eickhoff SB (2018) Towards a human self-regulation system: Common and distinct neural signatures of emotional and behavioural control. Neurosci Biobehav Rev 90:400–410.

Mansouri FA, Koechlin E, Rosa MGP, Buckley MJ (2017) Managing competing goals-a key role for the frontopolar cortex. Nat Rev Neurosci.

694 Mars RB, Jbabdi S, Sallet J, O'Reilly JX, Croxson PL, Olivier E, Noonan MP, Bergmann C, Mitchell AS,
695 Baxter MG (2011) Diffusion-weighted imaging tractography-based parcellation of the human
696 parietal cortex and comparison with human and macaque resting-state functional connectivity.
697 J Neurosci 31:4087–4100.

698 Mars RB, Passingham RE, Jbabdi S (2018) Connectivity Fingerprints: From Areal Descriptions to
699 Abstract Spaces. Trends Cogn Sci 22:1026–1037 Available at:
700 https://doi.org/10.1016/j.tics.2018.08.009.

701 Mars RB, Verhagen L, Gladwin TE, Neubert F-X, Sallet J, Rushworth MFS (2016) Comparing brains by
702 matching connectivity profiles. Neurosci Biobehav Rev 60:90–97.

703 Morawetz C, Bode S, Derntl B, Heekeren HR (2017) The effect of strategies, goals and stimulus
704 material on the neural mechanisms of emotion regulation: A meta-analysis of fMRI studies.
705 Neurosci Biobehav Rev 72:111–128 Available at:
706 http://www.sciencedirect.com/science/article/pii/S014976341630375X [Accessed June 22,
707 2017].

708 Motzkin JC, Philippi CL, Wolf RC, Baskaya MK, Koenigs M (2015) Ventromedial prefrontal cortex is
709 critical for the regulation of amygdala activity in humans. Biol Psychiatry 77:276–284.

710 Neubert F-X, Mars RB, Thomas AG, Sallet J, Rushworth MFS (2014) Comparison of human ventral
711 frontal cortex areas for cognitive control and language with areas in monkey frontal cortex.
712 Neuron 81:700–713.

713 Noback CR, Ruggiero DA, Demarest RJ, Strominger NL (2005) The human nervous system: structure
714 and function. Springer Science & Business Media.

715 Nolte J (1999) The human brain: an introduction to its functional anatomy. Mosby Inc.

716 Passingham RE, Stephan KE, Kötter R (2002) The anatomical basis of functional localization in the

717 cortex. Nat Rev Neurosci 3:606.

718 Petrides M, Pandya DN (2007) Efferent association pathways from the rostral prefrontal cortex in the
719 macaque monkey. J Neurosci 27:11573–11586.

720 Radke S, Roelofs K, De Bruijn ERA (2013) Acting on anger: social anxiety modulates approach-
721 avoidance tendencies after oxytocin administration. Psychol Sci 24:1573–1578.

722 Radke S, Volman I, Kokal I, Roelofs K, de Bruijn ERA, Toni I (2017) Oxytocin reduces amygdala
723 responses during threat approach. Psychoneuroendocrinology 79:160–166.

724 Radke S, Volman I, Mehta P, van Son V, Enter D, Sanfey A, Toni I, de Bruijn ERA, Roelofs K (2015)
725 Testosterone biases the amygdala toward social threat approach. Sci Adv 1:e1400074.

726 Ramnani N, Owen AM (2004) Anterior prefrontal cortex: insights into function from anatomy and
727 neuroimaging. Nat Rev Neurosci 5.

728 Ray RD, Zald DH (2012) Anatomical insights into the interaction of emotion and cognition in the
729 prefrontal cortex. Neurosci Biobehav Rev 36:479–501.

730 Ridderinkhof KR (2017) Emotion in action: A predictive processing perspective and theoretical
731 synthesis. Emot Rev 9:319–325.

732 Roelofs K, Cremers HR (2015) Cortical-amygdala decoupling during stress in patients with social
733 anxiety disorder. Biol Psychiatry 77:S298–S298.

734 Roelofs K, Minelli A, Mars RB, Van Peer J, Toni I (2008) On the neural control of social emotional
735 behavior. Soc Cogn Affect Neurosci:nsn036.

736 Roelofs K, van Peer J, Berretty E, de Jong P, Spinhoven P, Elzinga BM (2009) Hypothalamus–pituitary–
737 adrenal axis hyperresponsiveness is associated with increased social avoidance behavior in
738 social phobia. Biol Psychiatry 65:336–343.

739 Sallet J, Mars RB, Noonan MP, Neubert F-X, Jbabdi S, O'Reilly JX, Filippini N, Thomas AG, Rushworth
740 MF (2013) The organization of dorsal frontal cortex in humans and macaques. J Neurosci
741 33:12255–12274.

742 Semendeferi K, Teffer K, Buxhoeveden DP, Park MS, Bludau S, Amunts K, Travis K, Buckwalter J (2010)
743 Spatial organization of neurons in the frontal pole sets humans apart from great apes. Cereb
744 cortex 21:1485–1497.

745 Shekhar M, Rahnev D (2018) Distinguishing the Roles of Dorsolateral and Anterior PFC in Visual
746 Metacognition. J Neurosci 38:5078–5087 Available at:
747 http://www.jneurosci.org/lookup/doi/10.1523/JNEUROSCI.3484-17.2018.

748 Sheppes G, Scheibe S, Suri G, Radu P, Blechert J, Gross JJ (2014) Emotion regulation choice: a
749 conceptual framework and supporting evidence. J Exp Psychol Gen 143:163.

750 Tillman RM, Stockbridge MD, Nacewicz BM, Torrisi S, Fox AS, Smith JF, Shackman AJ (2018) Intrinsic
751 functional connectivity of the central extended amygdala. Hum Brain Mapp 39:1291–1312.

752 Tyborowska A, Volman I, Smeekens S, Toni I, Roelofs K (2016) Testosterone during puberty shifts
753 emotional control from pulvinar to anterior prefrontal cortex. J Neurosci 36:6156–6164.

754 Tzourio-Mazoyer N, Landeau B, Papathanassiou D, Crivello F, Etard O, Delcroix N, Mazoyer B, Joliot M
755 (2002) Automated anatomical labeling of activations in SPM using a macroscopic anatomical
756 parcellation of the MNI MRI single-subject brain. Neuroimage 15:273–289.

757 van Peer JM, Roelofs K, Rotteveel M, van Dijk JG, Spinhoven P, Ridderinkhof KR (2007) The effects of
758 cortisol administration on approach–avoidance behavior: an event-related potential study. Biol
759 Psychol 76:135–146.

760 van Peer JM, Spinhoven P, van Dijk JG, Roelofs K (2009) Cortisol-induced enhancement of emotional
761 face processing in social phobia depends on symptom severity and motivational context. Biol

762 Psychol 81:123–130.

763 Vendetti MS, Bunge SA (2014) Evolutionary and Developmental Changes in the Lateral Frontoparietal
764 Network: A Little Goes a Long Way for Higher-Level Cognition. Neuron 84:906–917 Available at:
765 http://www.ncbi.nlm.nih.gov/pmc/articles/PMC4527542/.

766 Volman I, Roelofs K, Koch S, Verhagen L, Toni I (2011a) Anterior prefrontal cortex inhibition impairs
767 control over social emotional actions. Curr Biol 21:1766–1770.

768 Volman I, Toni I, Verhagen L, Roelofs K (2011b) Endogenous testosterone modulates prefrontal–
769 amygdala connectivity during social emotional behavior. Cereb Cortex:bhr001.

770 Volman I, Verhagen L, den Ouden HEM, Fernández G, Rijpkema M, Franke B, Toni I, Roelofs K (2013)
771 Reduced serotonin transporter availability decreases prefrontal control of the amygdala. J
772 Neurosci 33:8974–8979.

773 Volman I, von Borries AKL, Bulten BH, Verkes RJ, Toni I, Roelofs K (2016) Testosterone modulates
774 altered prefrontal control of emotional actions in psychopathic offenders. ENeuro 3:ENEURO-
775 0107.

776 von Borries AKL, Volman I, de Bruijn ERA, Bulten BH, Verkes RJ, Roelofs K (2012) Psychopaths lack the
777 automatic avoidance of social threat: relation to instrumental aggression. Psychiatry Res
778 200:761–766.

779 Wager TD, Davidson ML, Hughes BL, Lindquist MA, Ochsner KN (2008) Prefrontal-subcortical
780 pathways mediating successful emotion regulation. Neuron 59:1037–1050.

781 Whiten A (2017) Culture extends the scope of evolutionary biology in the great apes. Proc Natl Acad
782 Sci 114:7790–7797 Available at: http://www.pnas.org/lookup/doi/10.1073/pnas.1620733114.

783 Whittle S, Yücel M, Yap MBH, Allen NB (2011) Sex differences in the neural correlates of emotion:
784 evidence from neuroimaging. Biol Psychol 87:319–333.

785 Zajkowski WK, Kossut M, Wilson RC (2017) A causal role for right frontopolar cortex in directed, but
786 not random, exploration. Elife 6.

787